Evaluating the Side Force in Oseen Flow Slender Body Theory and Comparison with CFD Simulation Results

Hamid M. Khan, Taimur A Shams and E. Chadwick

***Abstract*— The aerodynamic manoeuvring of slender bodies has been described by a new slender body theory developed by Chadwick. A higher value of side force has been calculated based on new Chadwick's model as compared to other theories. Four different slender models having elliptical cross-section with varying ellipticity were used to verify the new theory. The tests were conducted in a sub-sonic wind tunnel at optimized airstream velocity of thirty meters per second. The lift force was evaluated using experimental and CFD simulation methods with varying Angle of Attack (AoA) ranging between ±5 degrees in a way that the models were swiveled about the semi-major axis of the elliptical section. A comparison between the presented slender body theory, experiment and simulation is discussed.**

***Index Terms*— Oseen flow, slender body, side force, ellipticity**

I. Introduction

RECENTLY, a new approach is suggested by Chadwick which evaluates the additional viscous lift force. The theory describes the behaviour of slim bodies such as fuselage of aircraft, hull of ships and submarines [1] [2] [3]. The theory envisaged an increase in the side force on slender bodies when moving at a constant forward velocity. The bodies are considered to be moving at an AoA with respect to their symmetric axis. The side force thus evaluated has been observed to be more as compared to other slender body theories including Lighthill [4]. This approach evaluates the lift employing the concept of velocity extension expressed as oseenlets [5].

The successful verification of the new theory was conducted at the University of Salford. A subsonic wind tunnel was used to conduct the tests. The slender body models were produced using a 3-D printer. The tests were conducted at several steps to ensure the most appropriate attachment as well as the selection for the range test parameters. The special mount assembly has also been designed to minimize the flow separation at the nose section of the models. Model dimensions were chosen keeping in mind the wall effects of the wind tunnel and the flow regime to produce sufficient load balance response. The tests were funded through an EPSRC grant and the results have been published in the J. Fluid Mech. [6]. To further validate experimental results and extend the scope of investigation, the slender bodies were modelled for numerical studies. Computational Fluid Dynamics (CFD) method based on RANS type viscous flow solver was used to simulate the limited experimental cases. After satisfactory comparison of simulation results with the experimental data and theoretical predictions a couple of models were included for CFD simulations.

Manuscript received February 19, 2013.
Hamid M. Khan is with the National University of Sciences & Technology, Islamabad, Pakistan; (e-mail: h mehmood68@yahoo.com).
Taimur A. Shams is with the National University of Sciences & Technology, Islamabad, Pakistan (taimur12389@hotmail.com).
E. A. Chadwick is with the University of Salford, UK (e.a.chadwick@salford.ac.uk).

II. Experimental Setup

The work focuses on the study of slender bodies in Oseen flow and experimental verification of a new theory. The experimental results have also been compared with the CFD analysis. Experiments have been performed for four different bodies of varying ellipticity including 0, 12.5%, 25.0% and 37.5%. For comparison with the already existing data in the literature the slenderness ratio of the bodies used during the experiments was kept comparable with Jones' models [7]. The dimensions of the models were selected to satisfy the basic requirement of slender body theory. The length and the span of major axis were 0.8 m and 0.16 m respectively. The nose section of all models has 0.419 m radius of curvature extended up to first 0.25 m of length. Dimensions of the slender bodies have been restricted due to two reasons. For smaller sized slender bodies the issue was the sensitivity of the load balance of the wind tunnel, as it was incapable of capturing the response between one degree intervals in the AoA. The second restrain was the dimension of the test section of the wind tunnel. The bodies were made sufficiently large because they were by definition slender, but sufficiently small that it could fit into the working section of the wind tunnel without causing significant wall effects, figure 1.

Sheet metal of 3 mm thickness was used to make the initial slender body with zero ellipticity with approximate profile cut out for the nose section. The drawings of other slender bodies having 12.5%, 25.0% and 37.5% ellipticity respectively were made using Computer Aided Design (CAD). A rapid prototype 3-D printing machine was then used to convert the CAD drawings into slender bodies using Acrylonitrile Butadiene Styrene (ABS) thermoplastic. The 3-D printer made the model in four sections, labelled A, B, C and D. A slit was made in the sections of the model within which an aluminium plate of 0.003 m thickness having two

ISBN: 978-988-19252-9-9
ISSN: 2078-0958 (Print); ISSN: 2078-0966 (Online)

threaded holes was inserted for additional structural strength. Two mounts for support were also fastened to this plate at a distance of 0.26 m and 0.34 m from the nose respectively.

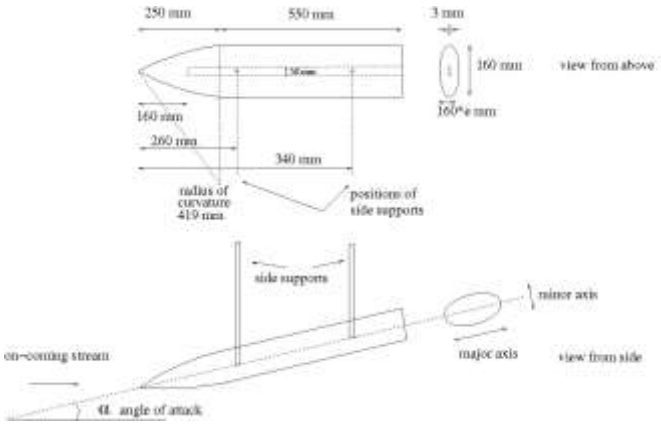

Fig. 1 - Lift force over angle range -5 to 5 for ellipticity 0.

Sheet metal of 3 mm thickness was used to make the initial slender body with zero ellipticity with approximate profile cut out for the nose section. The drawings of other slender bodies having 12.5%, 25.0% and 37.5% ellipticity respectively were made using Computer Aided Design (CAD). A rapid prototype 3-D printing machine was then used to convert the CAD drawings into slender bodies using Acrylonitrile Butadiene Styrene (ABS) thermoplastic. The 3-D printer made the model in four sections, labelled A, B, C and D. A slit was made in the sections of the model within which an aluminium plate of 0.003 m thickness having two threaded holes was inserted for additional structural strength. Two mounts for support were also fastened to this plate at a distance of 0.26 m and 0.34 m from the nose respectively.

III. Wind Tunnel

The experiments were conducted in a subsonic wind. The length, height and width of the cuboid section of the wind tunnel were 1.80 m, 1.15 m and 0.85 m respectively. A working speed of 30 meters per second was used to perform the tests. The downwash effects were considered to be negligible due to the slenderness of the model and small range of AoA. Moreover, the experimental data implies that the airstream interruption due to the mounts is insignificant. To minimize the chance of any uplift due to vortex shedding small range of AoA was used. The dimensions of the slender bodies were selected to maximise the acceptable length inside the test section of the wind tunnel along with permissible span to satisfy slender body theory, to facilitate recording of adequately reasonable experimental data by the load balance in the given range of AoA.

IV. CFD Analysis

During the experimental verification of the new theory the model dimensions were restricted due to sensitivity of the wind tunnel load balance and wall effects. These factors confined the size of slender bodies up to 37.5% ellipticity. The scope of the work was extended by conducting CFD analysis. For the validation of the experimental results the slender bodies were modelled in the CFD environment. ICEM-CFD was used for meshing and Fluent was used for the analysis. During the CFD analysis two different geometry models were made using the ANSYS Design Modeller Software. The models were made with varying ellipticity of 37.5% and 50%. The simulation results for 37.5% ellipticity model were used to compare with experimental results. The results were then used as a benchmark to run the simulations for 50% ellipticity model.

The total length of each model was 0.80 m, out of which nose section was 0.25 m. For both models the nose section consisted of nine parts, each part had an offset along z-axis. In both cases first the nose section was modelled and then the last part was extruded by 0.55 m to have full length of the body, figure 2. The boundary conditions play an important role in the accuracy of the CFD analysis. During this work a domain named “slender body” and four different boundary conditions were used. Tetra elements of 1.07 million and 1.053 million elements were used for 37.5% ellipticity and 50% ellipticity respectively. Domain and side view of mesh with domain for slender body model with 50% ellipticity are given in figures 3 and 4.

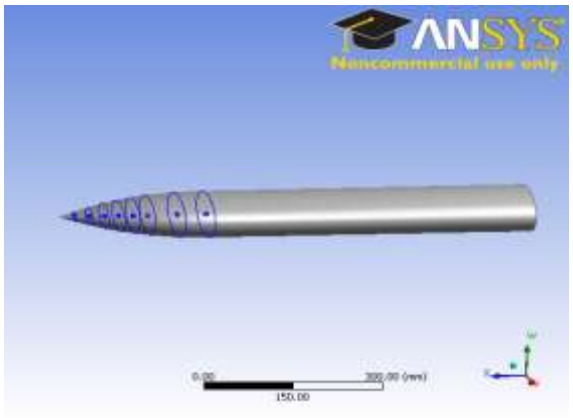

Fig 2 - Slender body model with 50% ellipticity and 0.80 m length.

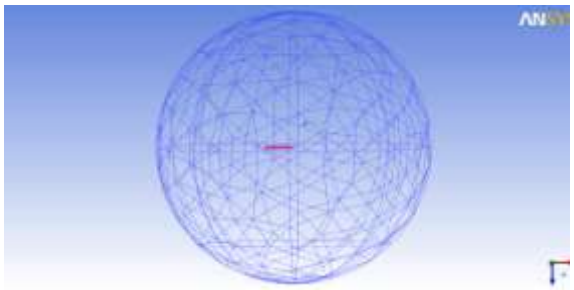

Fig 3 - Domain for slender body model with 50% ellipticity and 0.80 m length.

V. Results

The lift values obtained for a single run were normalized to obtain lift coefficient to present the experimental data for the slender body models. Mathematically, the coefficient of lift is calculated by dividing the lift force by the span of the body and dynamic pressure. But in case of slender bodies the span is very small due to the slimness, making the interpretation of results difficult. So, the Lighthill’s results from inviscid flow theory [4] have been used to bring in another coefficient of lift. According to this theory the lift force does not change significantly if the circle circumference of the end section has the similar radius

ISBN: 978-988-19252-9-9
ISSN: 2078-0958 (Print); ISSN: 2078-0966 (Online)

despite of the shape. The current study recommends that instead of using the base area the cross-sectional area of the circle that defines the end section of the slender body offers more meaningful coefficient of lift. The cross-sectional area of slender bodies used in this study is πs^2 where 's' is the span.

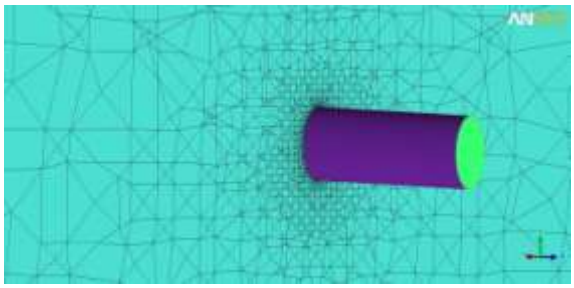

Fig 4 - Side view of mesh with domain for slender body model with 50% ellipticity and 0.80 m length.

The experimental data for side force (or lift) coefficient against AoA ranging between ±5 degrees were acquired for the models. A line of best fit is also plotted. Figures 5-8 represent the lift force ranging between ±5 degrees for models having 0, 12.5%, 25.0% and 37.5% ellipticity.

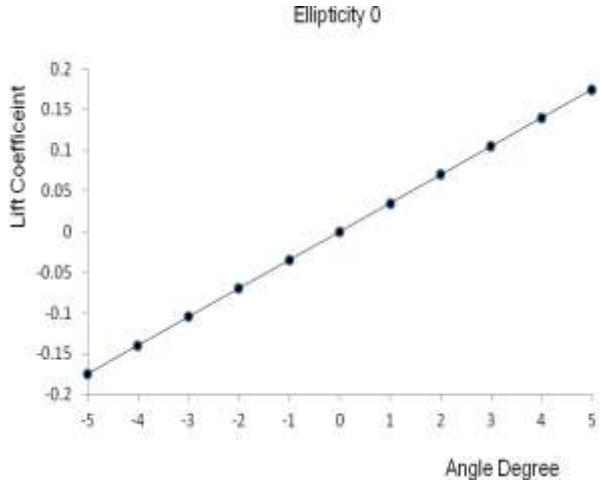

Fig. 5 - Lift coeffcient ranging between ±5 degrees for 0 ellipticity.

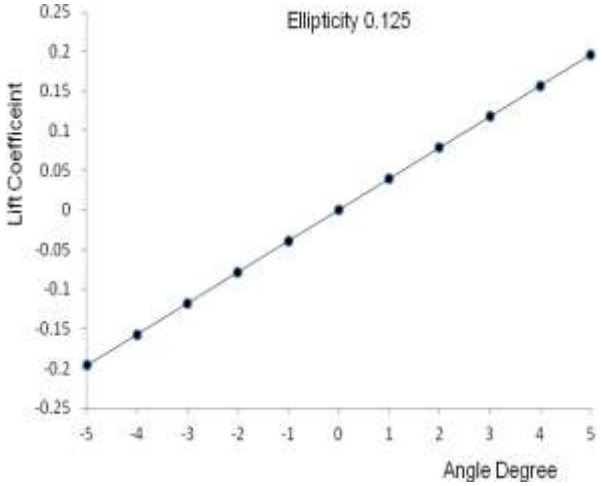

Fig. 6 - Lift coeffcient ranging between ±5 degrees for 12.5% ellipticity.

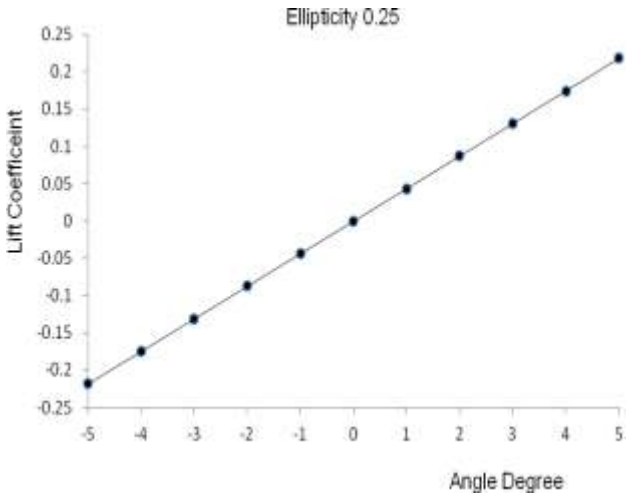

Fig. 7 - Lift coeffcient ranging between ±5 degrees for 25.0% ellipticity.

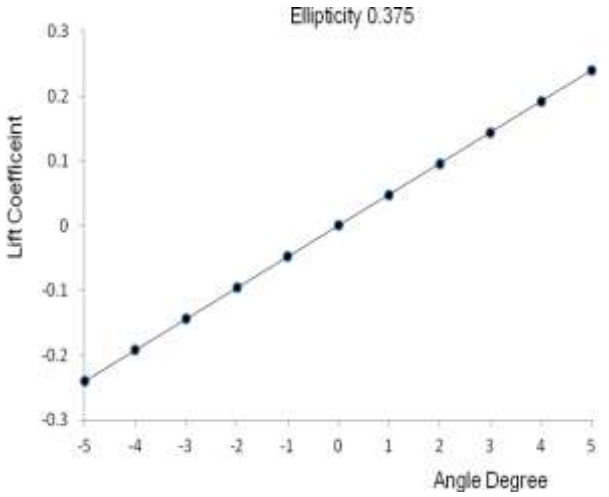

Fig. 8 - Lift coeffcient ranging between ±5 degrees for 37.5% ellipticity.

The CFD simulation results representing the lift force ranging between ±5 degrees for 37.5% and 50.0% ellipticity are plotted in figures 9 and 10 on next page.

ISBN: 978-988-19252-9-9
ISSN: 2078-0958 (Print); ISSN: 2078-0966 (Online)

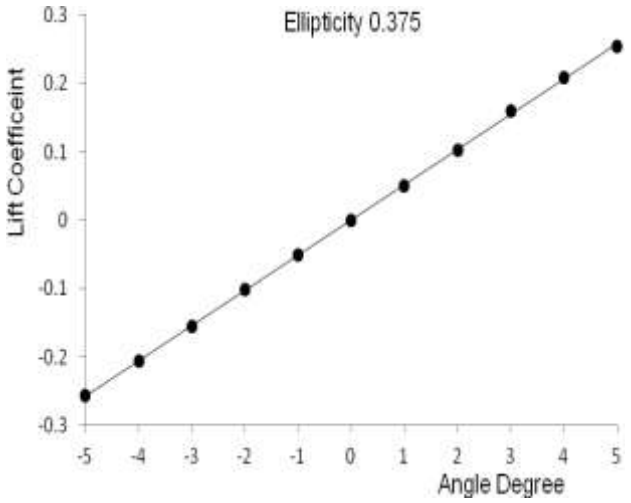

Fig. 9 - Lift coeffcient ranging between ±5 degrees for 37.5% ellipticity.

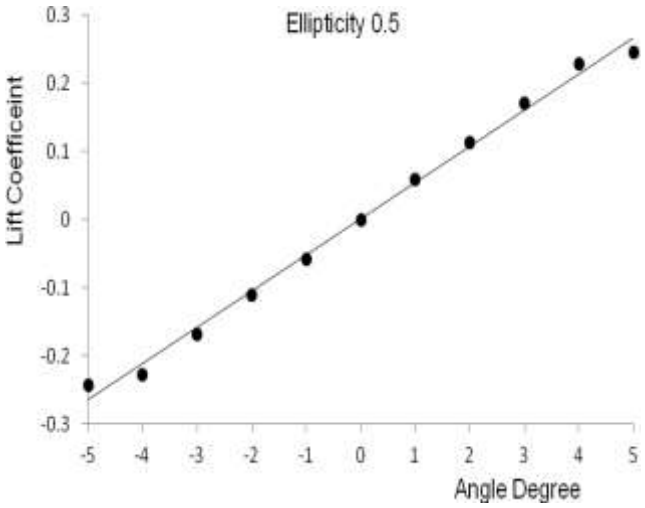

Fig. 10 - Lift coeffcient ranging between ±5 degrees for 50.0% ellipticity.

VI. Analysis of Results

The Oseen flow theory of [2] predicts the lift force for slender bodies with elliptical cross section inclined at angle of attack by rotating about the major elliptical axis as

$$L = \pi s^2 \rho U^2 a (1 + e)$$

and a lift coefficient of

$$C_L = 2 a (1+ e)$$

where 'e' is the ellipticity, and is described as the ratio of the semi-minor to the semi-major axis of the ellipse.

Using the experimental and simulation results, a comparison is made between experiments, CFD analysis and Chadwick's Oseen flow theory. It is shown that the experiments and simulation results present a linear trend following the Oseen theory. The set of experiments and CFD analysis for 37.5% ellipticity and simulation result for 50.0% ellipticity show a trend similar to the predicted result confirming the Oseen flow slender body theory, as shown in figures 11 and 12.

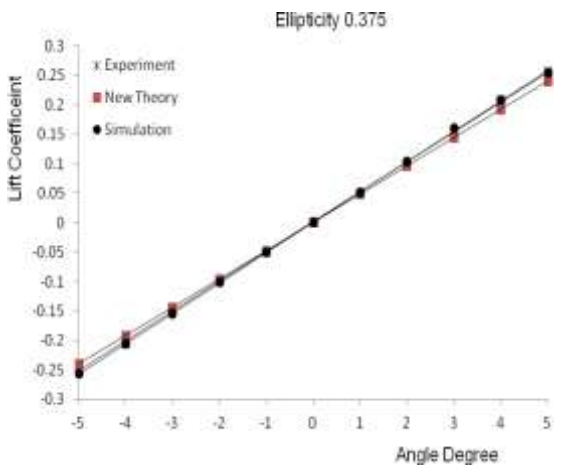

Fig. 11 - Comparison of lift coefficeint of experimental and simulation results with new theory ranging between ±5 degrees for 37.5% ellipticity.

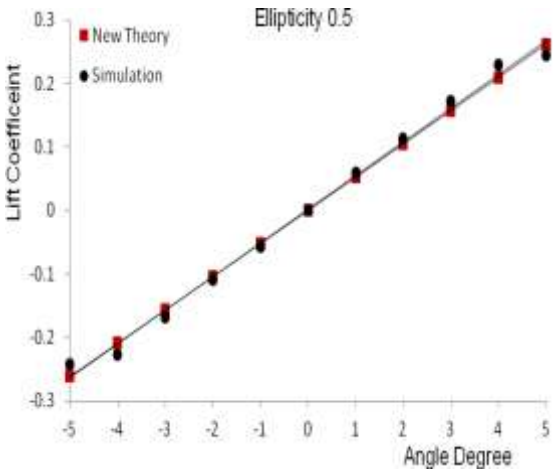

Fig. 12 - Comparison of lift coefficient of simulation results with new theory ranging between ±5 degrees for 50.0% ellipticity.

VII. Future Work

The new theory may be further developed by evaluating the coefficient of drag and moment. This requires an understanding of the forces, in particular side force, along the length of the slender body. Some experiments suggest a strong skewing of the side force towards the rear section of a slender body, especially the ship hulls. We would like to model slender bodies with different slenderness, and use CFD to capture vortex separation along the length to investigate the moment.

References

[1] E. Chadwick. A slender-body theory in Oseen flow. Proc. R. Soc. A, 458:2007-2016, 2002.
[2] E. Chadwick and N. Fishwick. Lift on slender bodies with elliptical cross section evaluated by using an Oseen flow model. SIAM. J. Appl. Math, 67(5):1465-1478, 2007.
[3] E. Chadwick. A slender body theory is Oseen flow obtained by expanding the Oseenlets in the Green's integral representation. Fluid Dyn. Resl, 41(045508): 17 pages, 2009.
[4] M.J. Lighthill. Note on the swimming of slender fish. J. Fluid Mech., 9:305-317, 1960.
[5] E.A. Chadwick, H. Khan, M. Mappin, M. Penney and M. Moatamedy. Experimental verification of an Oseen flow slender body theory. J. Fluid Mech., 654:271-279, 2010.
[6] Chadwick, E. (1998), The far field Oseen velocity expansion, Proc. R. Soc. A, 454, pp20592082.

ISBN: 978-988-19252-9-9
ISSN: 2078-0958 (Print); ISSN: 2078-0966 (Online)

[7] Jones, R. T. (1945), Properties of low-aspect-ratio pointed wings at speeds below and above the speed of sound, Nat. Adv. Comm. Aero., Report no. 835.

ISBN: 978-988-19252-9-9
ISSN: 2078-0958 (Print); ISSN: 2078-0966 (Online)